Acta Cryst B STRUCTURAL SCIENCE CRYSTAL ENGINEERING MATERIALS

ISSN 2052-5206

Effect of Al and Ca co-doping, in the presence of Te, in superconducting YBCO whiskers growth

Lise Pascale,[a] Marco Truccato,[b,c] Lorenza Operti[a,c] and Angelo Agostino[a,c]*

[a]Department of Chemistry and CrisDi Interdepartmental Center for Crystallography, University of Torino, via P. Giuria 7, Torino I-10125, Italy, [b]Department of Physics, University of Torino, via P. Giuria 1, Torino I-10125, Italy, and [c]NIS Centre of Excellence, University of Torino, Italy. *Correspondence e-mail: angelo.agostino@unito.it

Received 9 November 2015
Accepted 16 June 2016

Edited by P. Bordet, Institut Néel, France

Keywords: high-T_c superconductors; single-crystal X-ray diffraction; chemical doping; intrinsic Josephson junctions.

CCDC references: 1486062; 1486063

Supporting information: this article has supporting information at journals.iucr.org/b

High-T_c superconducting cuprates (HTSC) such as $YBa_2Cu_3O_{7-x}$ (YBCO) are promising candidates for solid-state THz applications based on stacks of intrinsic Josephson junctions (IJJs) with atomic thickness. In view of future exploitation of IJJs, high-quality superconducting YBCO tape-like single crystals (whiskers) have been synthesized from Ca–Al-doped precursors in the presence of Te. The main aim of this paper is to determine the importance of the simultaneous use of Al, Te and Ca in promoting YBCO whiskers growth with good superconducting properties (T_c = 79–84 K). Further, single-crystal X-ray diffraction (SC-XRD) refinements of tetragonal YBCO whiskers (*P*4/*mmm*) are reported to fill the literature lack of YBCO structure investigations. All the as-grown whiskers have also been investigated by means of X-ray powder diffraction (XRPD), scanning electron microscopy (SEM) and energy dispersive X-ray spectroscopy (EDS). Our results demonstrate that the interplay of Ca, Te and Al elements is clearly necessary in order to obtain superconducting YBCO whiskers. The data obtained from SC-XRD analyses confirm the highly crystalline nature of the whiskers grown. Ca and Al enter the structure by replacing the Y and the octahedral coordinated Cu1 site, respectively, as in other similar orthorhombic compounds, while Te does not enter the structure of whiskers but its presence in the precursor is essential to the growth of the crystals.

1. Introduction

Stacks of intrinsic Josephson junctions (IJJs) with atomic thickness are naturally present in layered high-T_c superconducting cuprates (HTSCs), such as $Bi_2Sr_2CaCu_2O_{8+x}$ (Bi-2212), $La_{2-x}Sr_xCuO_4$ (LSCO) and RE-123 (RE = Y, Eu, Gd, Dy, Ho, Er, Tm and Lu), as a result of their crystal structure (Kawae *et al.*, 2005; Kleiner *et al.*, 1992; Kubo *et al.*, 2008; Okutsu *et al.*, 2008). IJJs can be employed as modular elements in the realization of several cryogenic devices such as THz sensors in Wang *et al.* (2001) and emitters in Ozyuzer *et al.* (2007), micro-SQUIDs in Sandberg & Krasnov (2005) and quantum computers based on macroscopic quantum tunneling phenomena (Inomata *et al.*, 2005; Martinis *et al.*, 2005). Among the possible IJJ applications, high-frequency devices can take advantage of the large Josephson plasma frequency found in some HTSCs. In particular, $YBa_2Cu_3O_{7-x}$ (Y-123) has the highest Josephson plasma frequency, close to a few THz, because of its low anisotropy and high critical current density (Shibata & Yamada, 1997), which makes it a suitable candidate for the fabrication of these kinds of devices. Furthermore, such properties could be modulated, for instance, by chemical substitutions, as already noticed for Pb-doped Bi-2212 in Kambara *et al.* (2011). Within this context, we recently investigated the effect of different cationic substitutions

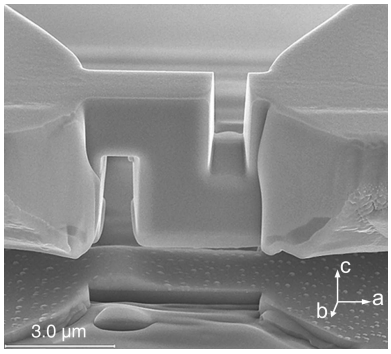

(Bertolotti *et al.*, 2014) of anionic doping (Rahman Khan *et al.*, 2009) and of X-ray nanobeam irradiation (Cagliero *et al.*, 2009; Pagliero *et al.*, 2014) on the electrical and structural properties of HTSC single crystals with high aspect ratios, also known as whiskers, belonging to Y-123 and Bi-2212 systems.

In view of the future exploitation of IJJs, whiskers are suitable structures for the study and the design of THz devices based on these junctions, which require a high homogeneity of properties on the micrometric scale. From this point of view, whiskers highly crystalline in nature, with excellent superconducting properties and low defect concentration represent crucial features for prototype fabrication. Moreover, starting from a micrometric cross section area, they are easily scalable by etching techniques down to submicrometric sizes and are also very suitable for three-dimensional machining, resulting in solid-state devices with a high degree of miniaturization (Inomata *et al.*, 2002; Kawae *et al.*, 2005; Okutsu *et al.*, 2008; Pavlenko *et al.*, 2009).

The growth of large amounts of Bi-2212 whiskers was reported soon after the discovery of HTSC in Matsubara *et al.* (1989) and has been extensively studied in Badica *et al.* (2006). On the other hand, with regard to Y-123, whiskers were first obtained much later only by making simultaneous use of both Te and Ca (Nagao *et al.*, 2003, 2004) in the precursor powders. Other growth strategies were investigated, for instance adding either Sb or Te as a single doping heteroelement (Nagao *et al.*, 2005, 2010), but with worse results. Ca-doping of Y-123 increases the carrier density of underdoped material (Awana *et al.*, 1994) as well as enhances both the values and the isotropy of the critical current density (Hammerl *et al.*, 2000; Rutter *et al.*, 2005), making Ca-doping essential for the YBCO whiskers growth. However, in just a few cases crystals have shown superconducting behavior and their yield always remained very limited. In our experiments, improving the work of Nagao *et al.* (2003, 2004, 2005, 2010), we have shown that the addition of limited amounts of Al_2O_3 powder to Ca-doped precursors, in the presence of Te, remarkably increases the amount of grown Y-123 whiskers. Therefore, we synthesized Al-doped $Y(Ca)Ba_2Cu_3O_{7-x}$ whiskers *via* a solid-state reaction method (Calore *et al.*, 2013).

To date, the influence of Ca-doping in Y-123 has been widely studied from the point of view of its crystal structure, both for polycrystalline material and for single crystals not grown with the whisker technique (Böttger *et al.*, 1997; Chen *et al.*, 2000; Hijar *et al.*, 1995). In principle, Ca should preferably substitute Y since the ionic radius of Ca^{2+} (r = 1.12 Å) is much closer to that of Y^{3+} (r = 1.019 Å) than to that of Ba^{2+} (r = 1.42 Å), and X-ray structure refinements of single crystals have shown that at low Ca concentrations (< 11%) Y^{3+} ions are actually substituted while, at higher concentrations Ca^{2+} also replaces Ba^{2+} (Böttger *et al.*, 1997).

Concerning the influence of Al doping on the structure and superconducting properties of YBCO, this topic has been studied by many authors both in polycrystalline samples, in bulk single crystals and in whiskers. For instance, this element was either incorporated from alumina crucibles used during the synthesis process or added in the form of Al_2O_3 nanoparticles to powders precursors, showing a substantial effect on the structure as well as the worsening of the transition temperature in both cases (Antal *et al.*, 2010; Franck *et al.*, 1987; Siegrist *et al.*, 1987).

To the best of our knowledge, no study has been carried out on the importance of the simultaneous presence of Al, Te and Ca in the precursors in promoting Y-123 whiskers growth with superconducting properties. Therefore, the present work is intended to underline the correlation of three such elements in the growth of YBCO whiskers by performing a comparison between Al-doped, simultaneously Ca- and Al-doped, Te- and Al-doped, and Ca-, Te- and Al-doped structures. Actually, it seems that tellurium oxide, in analogy with both aluminium and antimony oxides used as precursors, changes the phase diagram by creating mixed oxides, like $(BaCa)_3TeO_6$. This change in the phase diagram promotes the creation of a melting zone named 'microcrucible' according to the most accredited theories (Badica *et al.*, 2006), where the whiskers growth starts. Our experiments and related literature show how Sb and Te can increase the yield of whiskers as to Al (Nagao *et al.*, 2003, 2010; Calore *et al.*, 2013), without entering into the structure. While the superconducting properties of Y-123 whiskers have already been investigated to a good extent, the structural study has been inexplicably overlooked so far so that only a single-crystal X-ray diffraction (SC-XRD) refinement can be found in the literature reporting an orthorhombic YBCO structure (Bertolotti *et al.*, 2014). To fill this gap, in this paper we report SC-XRD refinements of tetragonal Y-123 whiskers. Moreover, all the as-grown crystals have been investigated by means of X-ray powder diffraction (XRPD), scanning electron microscopy (SEM) and energy dispersive X-ray spectroscopy (EDS). The superconducting properties have been evaluated and the resistivity measurements (R-T) are available as supporting information.

2. Experimental

2.1. Whiskers syntheses

In this work, doped single crystals (whiskers) of $YBa_2Cu_3O_{7-x}$ were grown according to a flux method. Through this process, high-quality crystals grow as a consequence of free nucleation from a high-temperature solid solution, where the flux is a mixture of oxides belonging to the Y–Ba–Cu–O phase diagram (Schneemeyer *et al.*, 1987; Sun *et al.*, 1990). Four different series of precursor powders were prepared by solid-state reaction from high-purity commercial Y_2O_3 (99.999%), $BaCO_3$ (99.9%), CuO (99.99%), $CaCO_3$ (99.95%), TeO_2 (99.995%) and Al_2O_3 (99.998%) (Sigma–Aldrich, Germany; Nagao *et al.*, 2003). Each precursor had a nominal cationic ratio of Y:Ba:Cu:Ca:Te:Al = 1:2:3:(0.0–1.0):0.5:(0.025–0.05) or 1:2:3:(0.0–1.0):0:0.05. Powders were thoroughly mixed and calcined for 3 h at 1073 K in air and in α-Al_2O_3 crucibles, with three intermediate grindings. Then the calcined powders were pressed into pellets of about 13 mm in diameter and 2 mm in thickness, which were subsequently put in a pure α-Al_2O_3 boat and placed in a tube furnace for the

Table 1
Synthesis identifier, nominal composition of precursors $YBa_2Cu_3Ca_uTe_vAl_wO_{7-x}$ (Ca = u, Te = v and Al = w), heat treatment conditions (T_{max} and T_{end}) and whisker results from different syntheses.

	$\alpha1$	$\alpha2$	$\beta1$	$\beta2$	$\gamma1$	$\gamma2$	$\gamma3$	$\delta1$
Ca = u	1	0.5	0	0	0.25	0.25	1	0
Te = v	0.5	0.5	0.5	0.5	0.5	0.5	0	0
Al = w	0.05	0.05	0.05	0.025	0.05	0.025	0.05	0.05
T_{max} (K)	1278	1253	1278	1278	1253	1278	1278	1278
T_{end} (K)	1178	1198	1198	1198	1198	1178	1198	1198
Whiskers	Y-123	Y-123	CuO	CuO	None	None	None	None

thermal treatment. The whisker growth was carried out by heating the pellets in a controlled oxygen flow of 0.1 L min^{-1} under a thermal cycle of T_{max} = 1253–1278 K, t_{dwell} = 5 h and T_{end} = 1178–1198 K, where T_{max} is the maximum temperature of the heating ramp, t_{dwell} is the dwell time at T_{max} and T_{end} is the end-point temperature of the cooling ramp after which the oven was turned off for furnace cooling. Differential thermal analysis (DTA) and power diffraction determinations were made on each series of precursors to define the best thermal conditions. All the syntheses were performed following the constant heating and cooling rates of 5 K min^{-1} and 1 K h^{-1}, respectively.

2.2. SEM/EDS analysis

In order to evaluate the surface morphology and the cationic stoichiometry of synthesized whiskers, some electron micrographs and energy dispersive spectrometer (EDS) measurements were performed by means of a Cambridge S-360 scanning electron microscope (SEM) equipped with an Oxford Inca Energy 200 EDS system and the INCA Oxford software.

2.3. Single-crystal X-ray diffraction

All crystal structures were investigated by single-crystal X-ray diffraction (SC-XRD). Intensities were collected at 293 K on an Xcalibur, Ruby, Gemini R Ultra diffractometer (Agilent Technologies UK Ltd), operating at 50 kV and 40 mA with graphite-monochromated Mo $K\alpha$ radiation, by using an ω-scan technique ($\Delta\omega$ = 1.0°). *CrysAlisPro* software has been used for data collection and reduction (peak intensities integration, background evaluation, cell dimensions and absorption correction; Agilent, 2012). Space-group determination, structure solution with direct methods (heavy-atom method) and refinement on F^2 have been performed by means of *JANA*2006 software (Petricek *et al.*, 2014). The refinements were done using harmonic atomic displacement parameters for all atoms, except O2 and O3 sites. The occupancy factors (OFs) of all crystallographic sites were refined taking in account all the possible atomic combinations. Only the proven substitution was reported. A numerical absorption correction was applied by a Gaussian integration method over the crystal shape.

2.4. Powder X-ray diffraction

Powder X-ray diffraction (XRPD) data were obtained by means of an X'Pert Panalytical powder diffractometer, equipped with a Cu target and an X'Celerator ultrafast line detector. The diffraction intensities were collected in a θ–θ

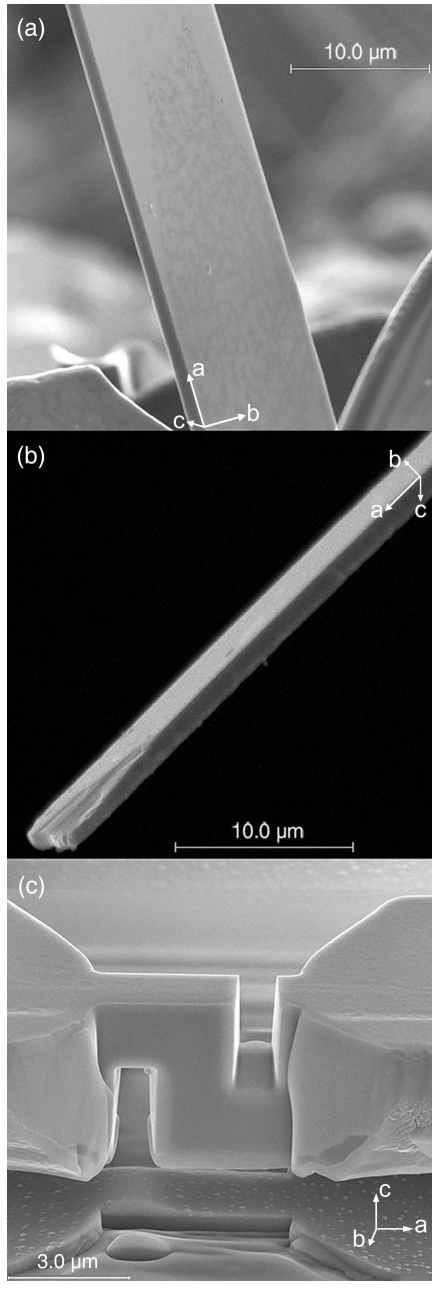

Figure 1
Scanning electron microscope (SEM) images of most common medium-sized Al-doped (Y,Ca)-123 whiskers obtained from batch (*a*) $\alpha1$ and (*b*) $\alpha2$. The surface structure is very regular whatever the nominal composition of the precursor. (*c*) An SEM picture of the YBCO micro-device investigated in our electrical study. This whisker, selected from batch $\alpha1$, has undergone different steps of micro-machining by means of a focused ion beam (FIB) instrument in order to fabricate stacks of intrinsic Josephson junctions. First, its cross-sectional area has been progressively decreased, then two trenches have been etched to force the current along the *c*-axis of the chip.

Table 2
Crystal data for single crystals $\beta1$ and $\beta2$, and for phase $\delta1$.

	$\beta1$	$\beta2$	$\delta1$ (Y-123)	$\delta1$ (Y-211)
Crystal system	Monoclinic	Monoclinic	Orthorhombic	Orthorhombic
Space group	*C*12/*c*1	*C*12/*c*1	*Pmmm*	*Pnma*
a, *b*, *c* (Å)	4.690 (1), 3.420 (1), 5.131 (1)	4.653 (3), 3.410 (1), 5.108 (2)	3.8303 (5), 3.8803 (5), 11.6669 (13)	5.6590 (1), 7.1325 (1), 12.1792 (2)
β (°)	99.54 (2)	99.48 (1)	90	90

geometry, with Cu $K\alpha$ radiation and an angular step size of 0.002°. Data analyses were performed using a Le Bail approach by means of the *JANA*2006 software.

3. Results and discussion

Table 1 summarizes the synthesis identifiers, the nominal composition of different precursors $YBa_2Cu_3Ca_uTe_vAl_wO_{7-x}$ employed, the experimental details (T_{max} and T_{end}) and the kind of whisker obtained from the various syntheses. First, we have been able to obtain Y-123 single-crystal whiskers only starting from the precursors $\alpha1$ and $\alpha2$, and these crystals turned out to be superconductors with T_c values of 79.8 and 83.8 K, respectively (*R versus T* measurements are available as supporting information). SEM analyses were performed in order to obtain a morphological characterization.

Fig. 1 shows some SEM micrographs for the $\alpha1$ (panel a) and $\alpha2$ (panel b) synthesis batches. Our doped-YBCO whiskers are characterized by a quite regular tape-like structure of $\sim$ 0.2–1 mm in length, grown with a preferential direction and with a flat plane surface 10–35 µm in width and 2–10 µm in thickness. In order to obtain information about the elemental composition, EDS measurements were also performed. From a qualitative point of view, this analysis allows us to state that all whiskers grown from starting batches $\alpha1$ and $\alpha2$ contain Y, Ba, Cu, O, Ca and Al but not Te. This outcome is in agreement with other similar compounds reported in Bertolotti *et al.* (2014) and Nagao *et al.* (2003). However, from a quantitative point of view, the evaluation of Al content could not be performed due to overlap of the corresponding peak with the Y $K\alpha$ one. The oxygen content could not be accurately determined either. Therefore, we could not define the corresponding stoichiometric compositions.

Data reported in Table 1 summarize the best conditions defined by DTA for each synthesis of YBCO after the variation of calcium in the stoichiometry. Some syntheses which failed significantly were also reported. During the experimental process, a decrease in nominal calcium content, *i.e.* from 1.0 in the $\alpha1$ precursor to 0.5 in the $\alpha2$ precursor, causes a reduction in the size of the obtained crystals. Probably the creation of intermediate oxide precursors, as $(BaCa)_3TeO_6$, is crucial to increase the crystal size of the whiskers. In fact, reducing the amount of Ca in the pellet (see $\gamma1$ and $\gamma2$ syntheses) means that the growth of whiskers is no longer detected. However, while removing it completely (see precursors $\beta1$ and $\beta2$), an anomalous and concurrent growth of CuO whiskers occurs. This clearly indicates the necessity of introducing Ca in the precursors in order to obtain YBCO whiskers. Moreover, it is noticeable that the content in Al, within the range of concentrations used in this paper, does not affect the type of whisker which we obtain, which can be Y-123 or CuO, or neither. What we observe instead is that the content in Al strongly influences the yield from the synthesis. Indeed, according to the Al content in the precursor, what varies is the number of nucleation centers present on the pellet, as explained by the 'microcrucible' model in Badica *et al.* (2012) and Boston *et al.* (2014), and therefore the final number of whiskers grown. With regard to Te, its presence in the precursor seems to be essential to the growth of whisker crystals since, when removed, we do not obtain any whisker and the resulting sintered precursor pellet shows the presence of YBCO polycrystalline material (see $\gamma1$, $\gamma2$ and $\gamma3$) or a mixed Y-123/Y-211 phase (see $\delta1$).

The CuO whiskers $\beta1$ and $\beta2$ were identified by means of SC-XRD, while the Y-123/Y-211 phase $\delta1$ was assigned by XRPD data. The crystal systems, space groups and lattice parameters of crystals $\beta1$, $\beta2$ and phase $\delta1$ are reported in Table 2.

Crystals $\alpha1$ and $\alpha2$ were structurally studied by SC-XRD. The experimental details of the refinements are given in Table 3. Atomic coordinates, equivalent isotropic displacement parameters obtained from single-crystal refinements and the list of interatomic distances are available as supporting information. Both crystals studied are characterized by a tetragonal non-stoichiometric stacked perovskite–rock salt–perovskite structure with space group *P*4/*mmm* (Z = 1), by similar lattice parameters and by similar atomic coordinations, but differ in the composition (notably Ca and Al) as well as in the doping content (O). Structure refinements converged at $R \simeq 0.020$ and $0.027 < wR < 0.038$.

3.1. Crystal $\alpha1$

Fig. 2 shows the tetragonal structure of crystal $\alpha1$. Y and Ba ions occupy the 1*d* (4/*mmm*) and the 2*h* (4*mm*) Wyckoff sites, respectively. Cu1, which is in the 1*a* (4/*mmm*) Wyckoff site, achieves an octahedral coordination geometry where four O3 ions (2*f* Wyckoff site, *mmm*) form the plane and two O1 (1*b* Wyckoff site, 4/*mmm*) form the vertices. Finally, the Cu2 ion occupies the 2*g* Wyckoff site (4*mm*) and has a slightly distorted square-pyramidal coordination, with four O2 ions (4*i* Wyckoff site, 2*mm*) in the plane and a weak interaction with apical O1.

Crystal $\alpha1$ is Ca- and Al-doped but Te-free. This result is in agreement with our EDS analysis and ICP-MS (ion-coupled plasma mass spectrometry) analysis previously reported in

Table 3
Experimental details: crystal data, data collection and structure refinements for the single crystals $\alpha1$ and $\alpha2$.

For all structures: $Z = 1$ and refinement was with 0 restraints. Experiments were carried out at 293 K with Mo $K\alpha$ radiation using an Xcalibur, Ruby, Gemini ultra diffractometer by using an ω-scan technique. Refinement was on 20 parameters.

	Crystal $\alpha1$	Crystal $\alpha2$
Crystal data		
Chemical formula	$Y_{0.95}Ca_{0.05}Ba_2Cu_{2.84}Al_{0.16}O_{6.75}$	$Y_{0.92}Ca_{0.08}Ba_2Cu_{2.90}Al_{0.10}O_{6.89}$
M_r	654.01	657.02
Crystal system, space group	Tetragonal, *P4/mmm*	Tetragonal, *P4/mmm*
a, c (Å)	3.8551 (3), 11.6782 (8)	3.8526 (5), 11.6660 (15)
V (Å^3)	173.56 (3)	173.15 (5)
$F(000)$	288.5	290
D_x (Mg m^{-3})	6.257	6.301
μ (mm^{-1})	27.61	27.65
Crystal size (mm)	0.29 × 0.02 × 0.01	0.23 × 0.02 × 0.01
Data collection		
Absorption correction	Gaussian integration	Gaussian integration
T_{min}, T_{max}	0.197, 0.811	0.127, 0.821
No. of measured, independent and observed [$I > 3\sigma(I)$] reflections	3779, 186, 174	1215, 186, 162
R_{int}	0.038	0.033
$(\sin\theta/\lambda)_{max}$ (Å^{-1})	0.683	0.683
Refinement		
$R[F^2 > 2\sigma(F^2)]$, $wR(F^2)$, S	0.021, 0.038, 1.52	0.020, 0.027, 0.92
No. of reflections	174	162
$\Delta\rho_{max}$, $\Delta\rho_{min}$ (e Å^{-3})	1.32, −1.45	0.47, −0.52

Computer programs: *CrysAlisPro* (Agilent, 2012), *JANA*2006, Version 28/04/2014 (Petricek *et al.*, 2014).

Bertolotti *et al.* (2014). The refinement was carried out allowing Ca^{2+} to replace both Y^{3+} and Ba^{2+} and, as in other similar compounds (Bertolotti *et al.*, 2014; Nagao *et al.*, 2003), only the Y^{3+} site is substituted by Ca^{2+} with a molar ratio Y^{3+}/Ca^{2+} of 0.95/0.05. This crystal also contains Al ions; the refinement shows that only Cu1 is substituted and the molar ratio Cu1/Al is 0.95/0.05. The OFs of all O atoms have been refined: only O3 has shown that the site occupancy is not full (OF = 0.38). The experimental formula of crystal $\alpha1$ is therefore $(Y_{0.95}Ca_{0.05})Ba_{2.00}(Cu_{2.84}Al_{0.16})O_{6.75}$.

The changes engendered in Y-123 whisker structure by Ca doping need to be discussed. Since the structural parameters of YBCO depend on the doping level as well as on the oxygen content, we have taken, as a reference from the literature, the data of an undoped tetragonal single crystal with a similar oxygen content (Okamura *et al.*, 1987). In this way, it is possible to separate the changes induced by Ca doping from those due to oxygen stoichiometry. The main effect of Y^{3+} (r = 1.019 Å) substitution by the larger Ca^{2+} (r = 1.12 Å) is an increase in the distance between the Cu2—O2 planes, separated by Y(Ca). Indeed, the atomic distance Cu2—Cu2 changes from 3.280 (7) Å in the undoped Y-123 to 3.3381 (5) Å in our $\alpha1$ Y(Ca)-123 whisker, taking Cu2 closer to the apical oxygen O1 [the distance Cu2—O1 is reduced from 2.529 (24) to 2.3512 (3) Å]. This effect has already been observed in other Y—Ba—Cu—O materials doped with Ca, as single crystals of YBCO (Böttger *et al.*, 1997), Y-247 and Y-124 (Schwer *et al.*, 1994), as well as in polycrystalline Y-123 (Böttger *et al.*, 1996).

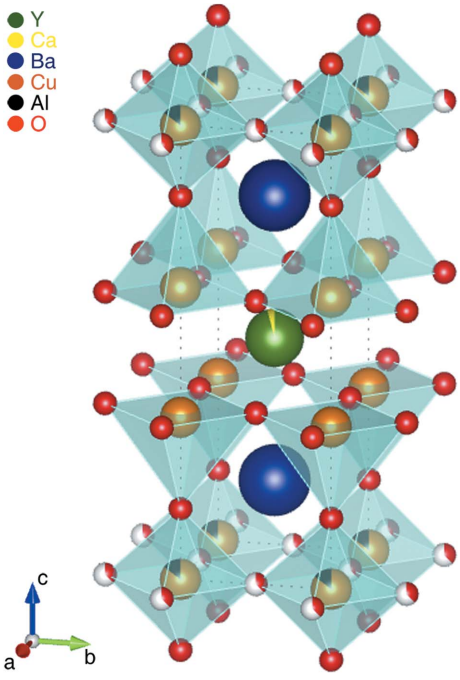

Figure 2
VESTA plot of the unit cell of crystal $\alpha1$, $(Y_{0.95}Ca_{0.05})Ba_{2.00}(Cu_{2.84}Al_{0.16})O_{6.75}$. Ca^{2+} partially occupies the Y site, while Al^{3+} the Cu1 position. The O3 site has non-unitary occupancy of 0.39.

3.2. Crystal $\alpha2$

The structure of crystal $\alpha2$ is very close to crystal $\alpha1$, as described above. The refinement shows that Ca^{2+} partially replaces Y^{3+}, while only the Cu1 ion is substituted by Al^{3+}. In this case, the molar ratios Y/Ca and Cu1/Al are 0.92/0.08 and 0.97/0.03, respectively. Contrary to what we could expect from the nominal composition of precursors (see $\alpha1$ and $\alpha2$ in Table 1), Ca content in this crystal is higher with respect to what we found in crystal $\alpha1$. However, Ca concentrations we used in both $\alpha1$ and $\alpha2$ pellets were, respectively, 4.6 and 9 times greater than the maximum Y/Ca replacement level found in single crystals of Ca-doped YBCO (Calore *et al.*, 2013). Furthermore, from both $\alpha1$ and $\alpha2$ single-crystal structure refinements, Ca was found to occupy only the Y site at low levels of doping (less than 11%). The occupancy of the O3 site has been refined to a value of 0.44, resulting in an experi-

mental formula for crystal $\alpha 2$ of $(Y_{0.92}Ca_{0.08})Ba_{2.00}(Cu_{2.90}Al_{0.10})O_{6.89}$.

4. Conclusions

High-quality superconducting YBCO-doped tape-like single crystals were grown from simultaneously Ca–Al-doped precursors, in the presence of Te. We observed that an increment of the Ca content in the structure causes a reduction of the length of the crystals. The addition of alumina in the precursor pellet strongly influences the yield of the synthesis but, at any content, the Al incorporation in the structure is nearly constant and occurs only at the Cu1 site. Finally, Te does not enter into the structure of whiskers but its presence in the precursor is essential to the growth of crystals (see the syntheses of $\gamma 1$, $\gamma 2$, $\gamma 3$ and $\delta 1$). Summarizing together these experimental results with the reported literature shows that the interplay of these three doping elements is clearly necessary in order to obtain Y-123 whiskers. Additional investigation is required to better understand the growth mechanism and shape formation of these singular micro-crystals.

The data obtained from SC-XRD analyses on as-grown samples confirm the highly crystalline nature of whiskers. All the examined crystals are characterized by a single tetragonal domain (*P*4/*mmm*). Ca and Al enter into the structure by replacing the Y and the octahedral coordinated Cu1 site, respectively, as in other similar orthorhombic compounds.

At present, further studies on the superconducting properties of these micrometric tetragonal doped-YBCO whiskers are in progress. The preliminary results are encouraging and offer new perspectives for future work on chemically induced IJJ modulation for the generation of materials with new functionalities.

References

Agilent (2012). *CrysAlisPro*, Version 1.171.36.28. Agilent Technologies UK Ltd, Oxford, England.

Antal, V., Zmorayová, K., Kováč, J., Kavečanský, V., Diko, P., Eisterer, M. & Weber, H. W. (2010). *Supercond. Sci. Technol.* **23**, 065014.

Awana, V. P. S., Tulapurkar, A., Malik, S. K. & Narlikar, A. V. (1994). *Phys. Rev. B*, **50**, 594–596.

Badica, P., Agostino, A., Khan, M. M. R., Cagliero, S., Plapcianu, C., Pastero, L., Truccato, M., Hayasaka, Y. & Jakob, G. (2012). *Supercond. Sci. Technol.* **25**, 105003.

Badica, P., Togano, K., Awaji, S., Watanabe, K. & Kumakura, H. (2006). *Supercond. Sci. Technol.* **19**, R81–R99.

Bertolotti, F., Calore, L., Gervasio, G., Agostino, A., Truccato, M. & Operti, L. (2014). *Acta Cryst.* B**70**, 236–242.

Boston, R., Schnepp, Z., Nemoto, Y., Sakka, Y. & Hall, S. R. (2014). *Science*, **344**, 623–626.

Böttger, G., Mangelschots, I., Kaldis, E., Fischer, P., Krüger, C. & Fauth, F. (1996). *J. Phys. Condens. Matter*, **8**, 8889–8905.

Böttger, G., Schwer, H., Kaldis, E. & Bente, K. (1997). *Physica C*, **275**, 198–204.

Cagliero, S., Piovano, A., Lamberti, C., Rahman Khan, M. M., Agostino, A., Agostini, G., Gianolio, D., Mino, L., Sans, J. A., Manfredotti, Ch. & Truccato, M. (2009). *J. Synchrotron Rad.* **16**, 813–817.

Calore, L., Rahman Khan, M. M., Cagliero, S., Agostino, A., Truccato, M. & Operti, L. (2013). *J. Alloys Compd*, **551**, 19–23.

Chen, C., Wondre, F., Chowdhury, A. J. S., Hodby, J. W. & Ryan, J. F. (2000). *Physica C*, **341–348**, 589–592.

Franck, J. P., Jung, J. & Mohamed, M. A. K. (1987). *Phys. Rev. B*, **36**, 2308–2310.

Hammerl, G., Schmehl, A., Schulz, R. R., Goetz, B., Bielefeldt, H., Schneider, C. W., Hilgenkamp, H. & Mannhart, J. (2000). *Nature*, **407**, 162–164.

Hijar, C. A., Stern, C. L., Poeppelmeier, K. R., Rogacki, K., Chen, Z. & Dabrowski, B. (1995). *Physica C*, **252**, 13–21.

Inomata, K., Kawae, T., Kim, S. J., Nakajima, K., Yamashita, T., Nagao, M. & Maeda, H. (2002). *Physica C*, **372–376**, 335–338.

Inomata, K., Sato, S., Nakajima, K., Tanaka, A., Takano, Y., Wang, H. B., Nagao, M., Hatano, H. & Kawabata, S. (2005). *Phys. Rev. Lett.* **95**, 107005.

Kambara, H., Kakeya, I. & Suzuki, M. (2011). *Physica C*, **471**, 754–757.

Kawae, T., Nagao, M., Takano, Y., Wang, H. B., Hatano, T. & Yamashita, T. (2005). *Physica C*, **426–431**, 1479–1483.

Kleiner, R., Steinmeyer, F., Kunkel, G. & Müller, P. (1992). *Phys. Rev. Lett.* **68**, 2394–2397.

Kubo, Y., Tanaka, T., Takahide, Y., Ueda, S., Okutsu, T., Islam, A. T. M. N., Tanaka, I. & Takano, Y. (2008). *Physica C*, **468**, 1922–1924.

Martinis, J. M., Cooper, K. B., McDermott, R., Steffen, M., Ansmann, M., Osborn, K. D., Cicak, K., Oh, S., Pappas, D. P., Simmonds, R. W. & Yu, C. C. (2005). *Phys. Rev. Lett.* **95**, 210503–210506.

Matsubara, I., Kageyama, H., Tanigawa, H., Ogura, T., Yamashita, H. & Kawai, T. (1989). *Jpn. J. Appl. Phys.* **28**, L1121–L1124.

Nagao, M., Kawae, T., Yun, K., Wang, H., Takano, Y., Hatano, T., Yamashita, T., Tachiki, M., Maeda, H. & Sato, M. (2005). *J. Appl. Phys.* **98**, 073903.

Nagao, M., Sato, M., Maeda, H., Yun, K. S., Takano, Y., Hatano, T. & Kim, S. (2003). *Appl. Phys. Lett.* **82**, 1899–1901.

Nagao, M., Sato, M., Tachiki, Y., Miyagawa, K., Tanaka, M., Maeda, H., Yun, K. S., Takano, Y. & Hatano, T. (2004). *Jpn. J. Appl. Phys.* **43**, L324–L327.

Nagao, M., Watauchi, S., Tanaka, I., Okutsu, T., Takano, Y., Hatano, T. & Maeda, H. (2010). *Jpn. J. Appl. Phys.* **49**, 033101.

Okamura, F. P., Sueno, S., Nakai, I. & Ono, A. (1987). *Mater. Res. Bull.* **22**, 1081–1085.

Okutsu, T., Ueda, S., Ishii, S., Nagasawa, M. & Takano, Y. (2008). *Physica C*, **468**, 1929–1931.

Ozyuzer, L., Koshelev, A. E., Kurter, C., Gopalsami, N., Li, Q., Tachiki, M., Kadowaki, K., Yamamoto, T., Minami, H., Yamaguchi, H., Tachiki, T., Gray, K. E., Kwok, W. K. & Welp, U. (2007). *Science*, **318**, 1291–1293.

Pagliero, A., Mino, L., Borfecchia, E., Truccato, M., Agostino, A., Pascale, L., Enrico, E., De Leo, N., Lamberti, C. & Martínez-Criado, G. (2014). *Nano Lett.* **14**, 1583–1589.

Pavlenko, V. N., Latyshev, Y. I., Chen, J., Gaifullin, M. B., Irzhak, A., Kim, S. J. & Wu, P. H. (2009). *JETP Lett.* **89**, 249–252.

Petricek, V., Dusek, M. & Palatinus, L. (2014). *Z. Kristallogr.* **229**, 345–352.

Rahman Khan, M. M., Cagliero, S., Agostino, A., Beagum, M., Plapcianu, C. & Truccato, M. (2009). *Supercond. Sci. Technol.* **22**, 085011.

Rutter, N. A., Durrell, J. H., Blamire, M. G., MacManus-Driscoll, J. L., Wang, H. & Foltyn, S. R. (2005). *Appl. Phys. Lett.* **87**, 162507.

Sandberg, M. & Krasnov, V. M. (2005). *Phys. Rev. B*, **72**, 212501.

Schneemeyer, L. F., Waszczak, J. V., Siegrist, T., van Dover, R. B., Rupp, L. W., Batlogg, B., Cava, R. J. & Murphy, D. W. (1987). *Nature*, **328**, 601–603.

Schwer, H., Kaldis, E., Karpinski, J. & Rossel, C. (1994). *J. Solid State Chem.* **111**, 96–103.

Shibata, H. & Yamada, T. (1997). *Physica C*, **293**, 191–195.
Siegrist, T., Schneemeyer, L. F., Waszczak, J. V., Singh, N. P., Opila, R. L., Batlogg, B., Rupp, L. W. & Murphy, D. W. (1987). *Phys. Rev. B*, **36**, 8365–8368.
Sun, B. N., Hartman, P., Woensdregt, C. F. & Schmid, H. (1990). *J. Cryst. Growth*, **100**, 605–614.
Wang, H. B., Wu, P. H. & Yamashita, T. (2001). *Phys. Rev. Lett.* **87**, 107002–107005.